Materials Research. 2019; 22(5): e20190228
DOI: http://dx.doi.org/10.1590/1980-5373-MR-2019-0228

Green synthesis and Characterization of ZnO-$CoFe_2O_4$ Semiconductor Photocatalysts Prepared Using Rambutan (*Nephelium lappaceum* L.) Peel Extract

***Rahmayeni*[a]*, *Aimi Alfina*[a], *Yeni Stiadi*[a], *Hye Jin Lee*[b], *Zulhadjri*[a]**

[a]*Chemistry Department, Mathematics and Natural Sciences Faculty, Andalas University, Kampus Limau Manis, Padang, 25163, Indonesia*
[b]*Department of Chemistry and Green Nano Materials Research Center, Kyungpook National University, 80 Daehakro, Buk-gu, Daegu-city, 41566, Republic of Korea*

Received: March 11, 2019; Revised: July 01, 2019; Accepted: August 05, 2019

In this work, the semiconductor of ZnO-CoFe2O4 composites were prepared by green synthesis approach using rambutan peel extract (*Nephelium lappaceum* L.) as a capping agent. X-ray diffraction patterns of composites showed the main peaks of ZnO at 2θ = 31.8°, 34.5°, and 36.2° corresponding to hexagonal wurtzite structure and weak peak at 2θ = 35.4° for cubic structure of CoFe2O4. The formation of rice-like and small granular morphology were confirmed by scanning electron microscope (SEM) and transmission electron microscope (TEM), whereas the superparamagnetic behavior of the samples were determined by vibrating sample magnetometer (VSM). The spectrum of Fourier transform infrared (FTIR) and x-ray photoelectron spectroscopy (XPS) showed absorption bands related to a number of interactions and binding energy in the samples respectively. The photocatalytic performance of composites under solar light was evaluated for the degradation of Direct Red 81 and the dye from washing water of batik garments. The composites showed good photocatalytic activity with the degradation percentage reaching 99.6% for Direct Red 81 dye after 2 hours.

Keywords: *Hydrothermal, ZnO-$CoFe_2O_4$, rambutan, magnetic, degradation, Direct Red 81.*

1. Introduction

Recently, heterogeneous photocatalysts have received much attention due to their ability to eliminate dye molecules from wastewater economically, simply and thoroughly. ZnO semiconductors are in great demand and often used as the materials for photocatalytic processes due to environmentally friendly material and non-toxic, large abundance, and have great properties such as high chemical stability and photosensitivity[1,2]. However, ZnO has a fairly wide band gap (3.2 eV), so that it absorbs UV in a good capability but is limited in the visible region[3]. Therefore, the modified ZnO is needed to improve its ability to absorb visible light. One of the most common modifications is doping ZnO with metal oxide materials so called ferrite spinel $CoFe_2O_4$ forming of ZnO/$CoFe_2O_4$ composite. This magnetic material has small band gap which shows a potential ability to absorb light in the visible region. In addition, if the composites used in the catalytic process, it can be easily separated from a liquid solution using an external magnetic field due to their magnetic behavior[4].

Various methods have been developed to synthesize ZnO/$CoFe_2O_4$. For example, a high temperature hydrolysis of chelated zinc diethylene glycol alkoxide complexes in alkaline diethylene glycol solution[5] and hydrothermal technique with carbon nano spheres as the template[6]. The other methods include microwave combustion[7], co-precipitation[8], sol-gel process followed by hydrothermal treatment[9], and combustion reaction[10]. However, these methods require long time reaction, complex equipment, using chemicals, and high temperature, thus contributing to some negative effects on the environment. Therefore, it would be a great benefit to investigate another synthesis method which is environmentally friendly, easy, and inexpensive. Green synthesis is an alternative way to prepare eco-friendly materials since it uses non-hazardous ingredients such as natural materials and other non-toxic components. A promising approach for green synthesis is a hydrothermal technique because it uses water as a solvent and natural leaf extracts from plants such as *Camellia sinensis*[11], *Aloe vera*[12] *Azadirachta indica*[13], and *Solanum nigrum*[14] as capping agents which control the nanostructures of the desired particles. Another natural ingredient that has been used as a capping agent to synthesis NiO nanocrystals is peel extract from rambutan (*Nephelium lappaceum* L.) which is a tropical fruit belonging to the *Sapindaceae* family and closely related to lychees and longan[15, 16].

In this paper, ZnO-$CoFe_2O_4$ semiconductor magnetic materials were synthesized hydrothermally using rambutan peel extract as a capping agent aimed to control the formation of nanostructures. The advantages of this method are the use of low cost, non-toxic and environmentally sympathetic precursors, simple, and saving the procedure time. The major component in rambutan peel extract is phenolic compounds which functions as a capping agent, stabilizing and even chelating agents for capturing the metal ions and control the formation of nanostructures.

*e-mail: rahmayenni@sci.unand.ac.id

The effect of capping agent toward ZnO-$CoFe_2O_4$ composite can be observed through its morphology which is more homogeneity and smaller in particles size compared to that of (9) and (15). The activities in the catalytic process of the samples were investigated by monitoring of the degradation of Direct Red 81 (DR81: $C_{29}H_{19}N_5Na_2O_8S_2$) and dye from washing water of batik cloth in direct sunlight. Several parameters that affect the catalysis process were also analyzed.

2. Experimental Procedure

2.1 Materials

Chemicals were purchased from Merck and used without further purification. $Zn(NO_3)_2.4H_2O$, $Co(NO_3)_2.6H_2O$, $Fe(NO_3)_3.9H_2O$, ethanol, NaOH, and distilled water were used in preparation of the samples. Direct Red 81 (DR81) solution and liquid waste containing dyes from batik cloth were used as dyes.

2.2 Preparation of rambutan peel extract

The rambutan ((*Nephelium lappaceum* L.) fruit used in this study was the Terang Bulan variety from Pekanbaru, Indonesia. Rambutan peel was cut into small pieces, washed with water and then dried in oven at 50 ℃. A total of 3 grams of dried rambutan peel was mixed with 40 mL of distilled water and 20 mL of ethanol and then stirred while heated at 80 ℃ for 10 minutes. The mixture was filtered, and the filtrate was stored at 4 ℃ before used.

2.3 Synthesis of $CoFe_2O_4$ precursors

The synthesis of the $CoFe_2O_4$ precursors using a hydrothermal method and rambutan extract was as follows: stoichiometric amounts of cobalt nitrate $Co(NO_3)_2.6H_2O$ and ferric nitrate $Fe(NO_3)_3.9H_2O$ were mixed in 40 mL of diluted rambutan peel extract (80:20 distilled water : extract) and stirred (500 rpm). NaOH solution (4 M) was added drop-wise until the pH reached 12 and the suspension was stirred vigorously for another 30 minutes. After that, the suspension was transferred into a teflon-lined stainless steel autoclave and heated in an oven at 180℃ for 3 h. The precipitate was filtered, washed with distilled water until the pH reached 7, and then dried in the oven at 105 ℃. The product of $CoFe_2O_4$ (CoEN) was stored in glass vials at room temperature for further analysis.

2.4 Synthesis of ZnO-$CoFe_2O_4$ nanocomposites

The synthesis of ZnO-$CoFe_2O_4$ nanocomposites was conducted using a green synthesis approach and hydrothermal methods in the presence of diluted rambutan peel extract (80:20 distilled water:extract) as a capping agent. Three ZnO-$CoFe_2O_4$ nanocomposites (ZCoEN, ZCoENK, and ZCoE) were synthesized as follows: the ZCoEN sample was synthesized by adding 20 mmol of $Zn(NO_3)_2.4H_2O$ and $CoFe_2O_4$ nanoparticles (in mole ratio of 1:0.05) to 40 mL of diluted rambutan peel extract. The mixture was stirred at 500 rpm, then the pH was adjusted to 12 by drop-wise addition of NaOH solution (4M) and the suspension was stirred vigorously for 30 minutes. The suspension was subsequently transferred into a teflon-lined stainless steel autoclave and then heated in an oven at 180 ℃ for 3 h. After cooling to room temperature the precipitate was washed several times until the pH reached 7, and dried at 105 ℃ for 2 h. The ZCoE sample was synthesized as described for ZCoEN but without the addition of NaOH. ZCoENK samples were synthesized as described for ZCoEN followed by calcination at 500 ℃ for 3 h.

***2.5** Materials Characterization*

X-ray diffraction (XRD) measurements were conducted using a XRD Philips X'pert PAN PW3040 analytical diffractometer operating with Cu Kα radiation (λ=1.5406 A) in the 2θ range of 10-100°. The scanning electron microscope (SEM) images were acquired on a SEM, JEOL JSM-6360LA electron microscope under high vacuum condition. The detailed morphology of the samples was investigated by transmission electron microscope (TEM, JEM-1400). Magnetic properties of the samples were investigated by vibrating sampler magnetometer (VSM OXFORD 1.2H). The band gap energy (Eg) was determined using a diffuse reflectance UV-Vis spectrophotometer (Shimadzu UV-Vis 2450). Fourier transformed infrared (FT-IR) spectra were obtained by a FT-IR Thermo Nicolet iS5 using the KBr pellet technique. X-ray photoelectron spectroscopy (XPS ULVAC-PHI Quantera SXM) was used to determine the bending energy.

2.6 Photocatalytic Evaluation

Photocatalytic activities were evaluated by photodegradation of DR81 under the solar light irradiation. In a typical experiment, 20 mg composite photocatalysts were added into 20 mL of DR81 dye solution (25 mg L^{-1}) and the reaction was immediately placed under solar light irradiation for 2 h. At the end of incubation period, the volume of reaction mixture was restored to its starting volume by adding distilled water to replace the loss due to evaporation. Then, the photocatalysts were separated from the liquid and the residual DR81 concentration was determined by measuring the absorbance of the sample at 527 nm. The degradation percentage of DR81 can be calculated according to following equation[16, 17]:

$$\text{Degradation}(\%) = \frac{A_o - A_t}{A_o} \text{x } 100\% \qquad (1)$$

Where A_o is the initial concentration of the dye, A_t is the concentration at time *t*. As a control, the DR81 solution without photocatalysts was also irradiated for the same time. The optimal condition were determined by varying the dye concentration, irradiation time, and amount of catalyst.

3. Results and Discussion

3.1 Structural Analysis

X-ray diffraction (XRD) is a very useful tool to determine the phase, crystallinity, and purity of samples. Crystallite size of polycrystalline material was calculated using the Scherer formula:

$$D = 0.9\lambda/\beta \cos\theta \quad (2)$$

Where *D* is the crystallite size, λ is the wavelength of incident X-rays, θ is the Bragg diffraction angle and β is the full width at half maximum (FWHM) XRD peak of particles[18]. Figure 1 shows the XRD pattern of the samples synthesized by the green synthesis method using rambutan peel extract as a capping agent. The XRD pattern of the CoEN sample shows the specific peaks at 2Θ = 30.1°, 35.4°, 57.0°, 62.6° according to the ICSD standard code 109045 for spinel type of $CoFe_2O_4$. The composites of ZCoEN and ZCoENK show a sharp and specific peaks dominated by the peaks of ZnO at 2Θ = 31.8°, 34.5°, 36.2°, 56.6°, 62.9°, 66.4°, 68.0°, and 69.1°, corresponding to hexagonal wurtzite structure of ZnO (ICDD standard No. 01-078-3325). The peaks of cobalt ferrite do not appear clearly because of its low concentration in the composite, however for ZCoE sample, ferrite peaks appear quite clear. On the other hand, the peak of ZnO is not obvious because the sample is amorphous. The average crystallites size of ZCoEN and ZCoENK calculated using the Debye-Scherer equation were found to be 24.02 and 27.88 nm, respectively.

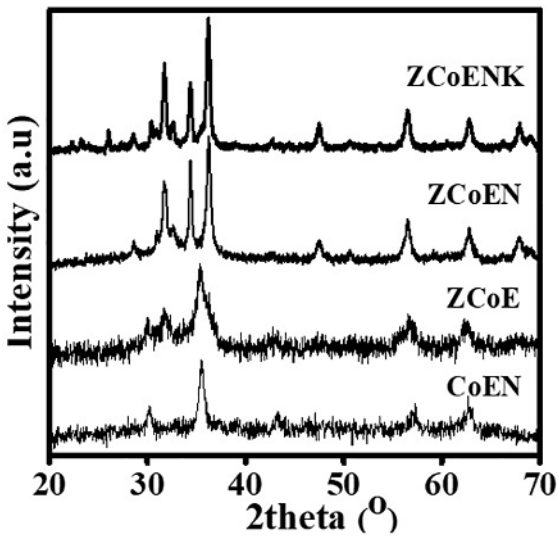

Figure 1. XRD patterns of CoEN, ZCoE, ZCoEN, and ZCoENK

3.2 Morphology

The surface morphology of two nanocomposite samples (ZCoEN and ZCoENK) were studied by scanning electron microscope (SEM) as shown in Figure 2. The images show that ZCoEN sample is composed with nanoparticles in the form of rice-like grains (Figure 2a), whilst ZCoENK sample comprises homogeneous fine grains (Figure 2b).

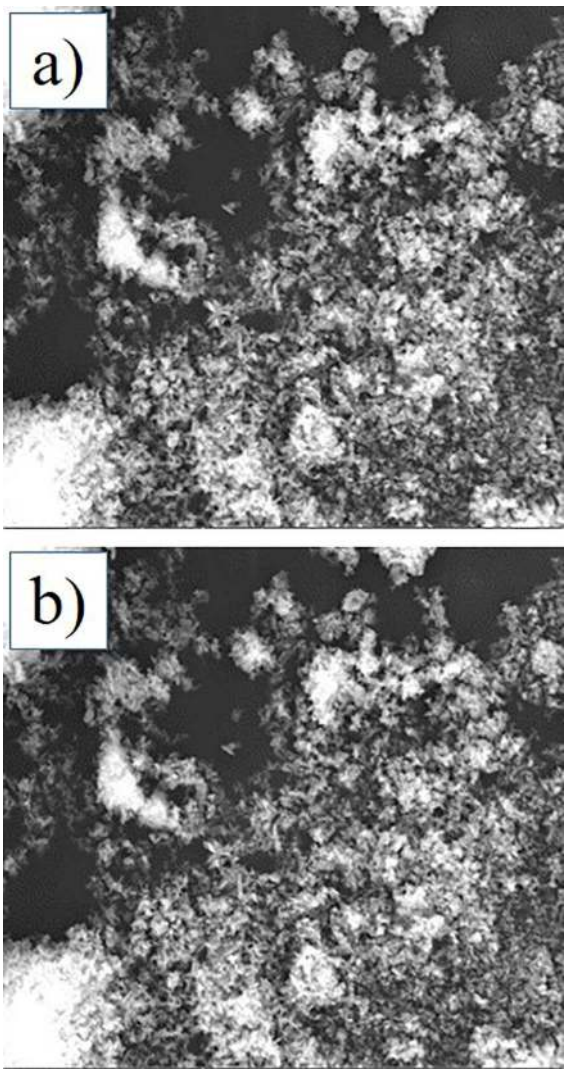

Figure 2. SEM images of (a) ZCoEN and (b) ZCoENK

Further morphological analysis was carried out using transmission electron microscopy (TEM) (Figure 3). TEM image reveals clearly the nanoparticles of $CoFe_2O_4$ (black part) are coated with ZnO (white part) forming a core and shell structure respectively. This structure facilitates electron transfer in composite (between $CoFe_2O_4$ and ZnO) and gives the benefit to the photocatalytic process.

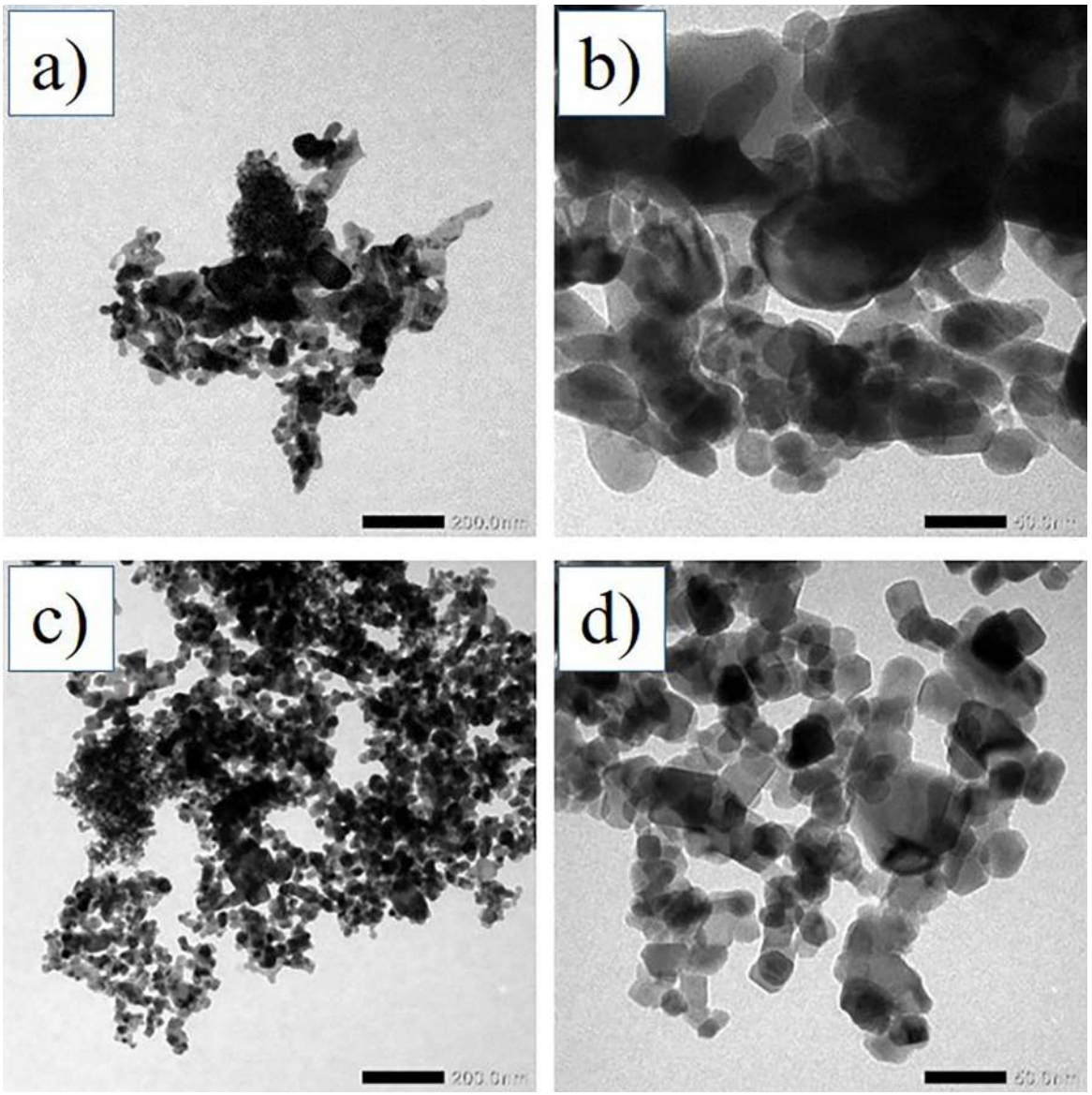

Figure 3. TEM image of ZCoEN (a, b) and ZCoENK (c, d)

The ZCoENK particles have cube-like shape with an average size of 25 nm while ZCoEN is larger in size compared with ZCoENK. The larger size of ZCoEN particles is probably due to the presence of organic compounds derived from the rambutan extract in the composite sample. On the other hand, the calcination in ZCoENK sample would release the organic compounds and leave empty space (pores) so that the particles become smaller. The smaller particle size should enhance the usefulness of this material as a photocatalyst.

3.3 VSM and DRS UV-Vis Analysis

The magnetic hysteresis curve of ZCoEN and ZCoENK are shown in Fig. 4a and 4b, respectively. The shape of the curves show that both samples have superparamagnetic properties with saturation magnetization (Ms) values of 12.1 emu/g for ZCoEN and 1.005 emu/g for ZCoENK, while the coercive field (Hc) values were 0.0095 T for ZCoEN and 0.011 T for ZCoENK. Magnetic properties of the samples in this present work were smaller than the sample reported by Sathishkumar et al.[8]. The ZCoENK composite has smaller particle size than ZCoEN which decreases the magnetic properties of this composite. Nevertheless, the magnetic properties of these smaller particles are still sufficient for easy recovery using an external magnetic field.

UV–Vis diffuse reflectance measurements were carried out to study the optical properties of the nanocomposites. Figure 4c and 4d show the DRS UV-Vis absorption spectra of the ZCoENK and ZCoEN composites, indicating the samples absorb light in the visible region. ZnO itself absorbs well in the UV region but only slightly in the visible region, while $CoFe_2O_4$ absorbs well in the visible region.

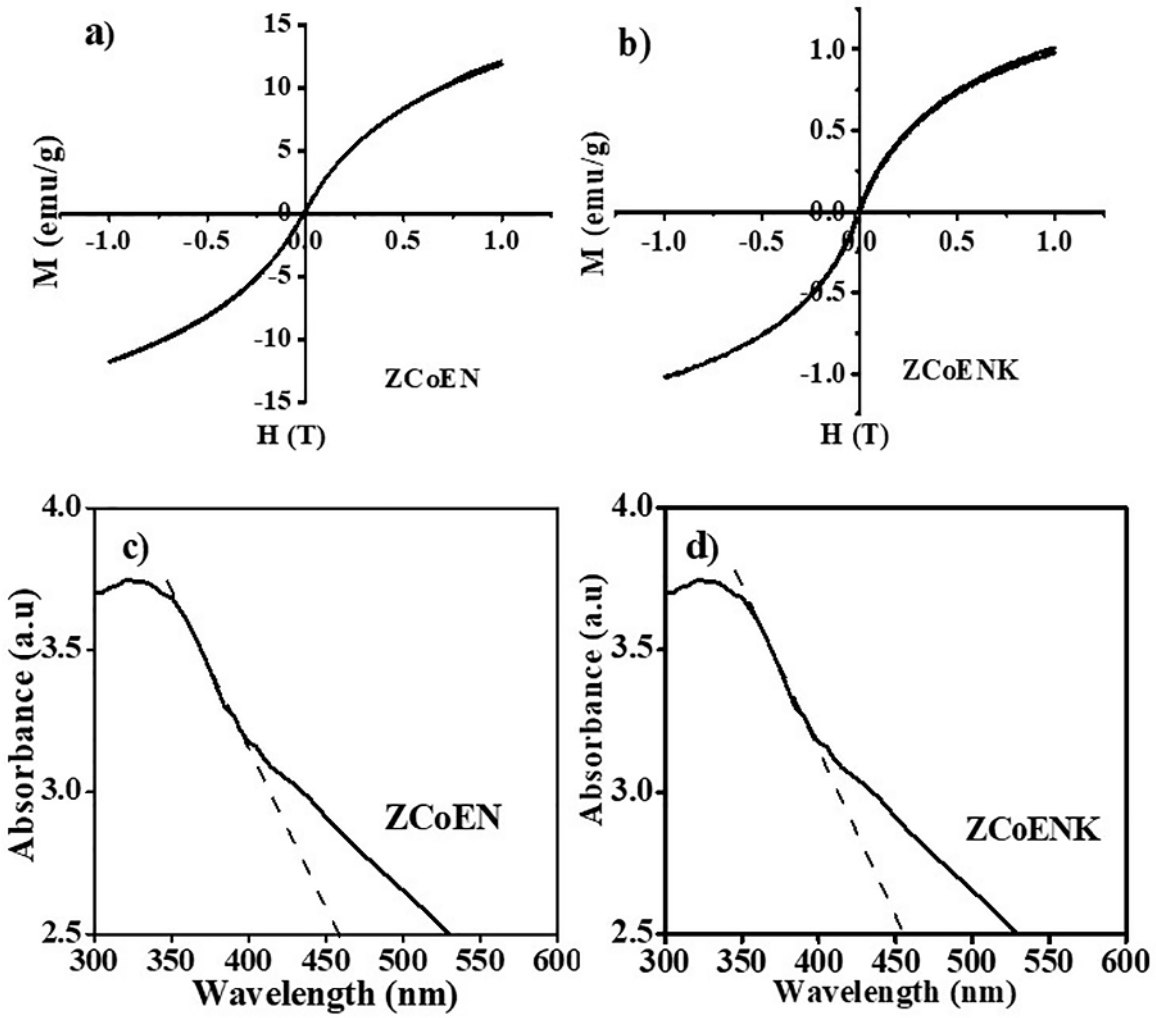

Figure 4. Hysteresis curve (a-b) and DRS UV-Vis spectra (c-d) of ZCoEN and ZCoENK

The combination of ZnO and $CoFe_2O_4$ produce a composite that can absorb in the visible region[8]. Therefore, these composites can be used as a catalysts for photocatalytic processes using sunlight. The band gap value is calculated using the follow equation:

$$Eg = hc/\lambda = 1240/\lambda \text{ eV} \quad (3)$$

where, Eg is the band gap energy (eV), h is Plank's constant (6.626×10^{-34}Js), c is the light velocity (3×10^8 ms^{-1}) and λ is the wavelength (nm) [16, 19]. From calculation, the band gap energy for the two composites is equal to 2.7 eV, lower than ZnO (~3.2 eV) but higher than $CoFe_2O_4$ (~1.6 eV). The decreasing of ZnO band gap with the presence of $CoFe_2O_4$ is due to the formation of ZnO-$CoFe_2O_4$ heterojunction semiconductors with type II band alignment when the ZnO and $CoFe_2O_4$ are coupled together forming core-shell[20]. The electrons and holes can be driven to opposite directions and physically separated, thus minimizing their recombination and could decrease the band gab of ZnO, and the material can be used as a photocatalysts in visible and solar light irradiation.

3.4 FTIR Analysis

The possible interaction between ZnO and $CoFe_2O_4$ in the samples was investigated by FTIR spectroscopy. The FTIR spectra of the samples are shown in Figure 5. The sharp peaks around 556 and 454 cm^{-1} are attributed to stretching vibration of the Fe-O and Co-O bond for spinel ferrite CoEN. The sharp peaks around 546 cm^{-1} are attributed to stretching vibration of the Fe-O bond and the peaks around 410-432 cm^{-1} to stretching vibration of Zn-O and Co-O in the three composite samples. The combination of ZnO and $CoFe_2O_4$ generates a shift in the absorption area for Zn-O and Fe-O bonds. The peaks around 350 cm^{-1} correspond to the M-O vibration[21-22].

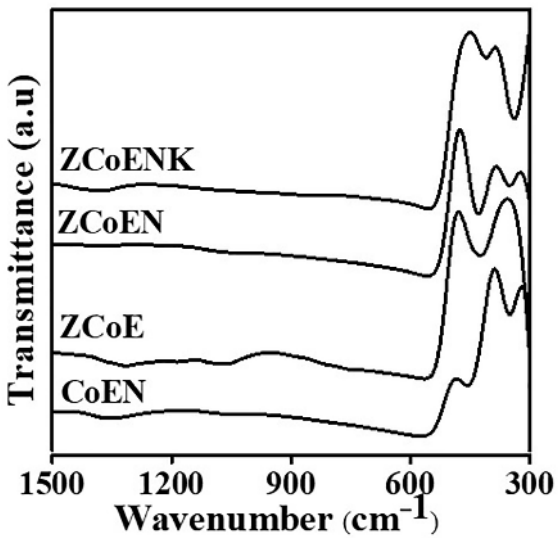

Figure 5. FT-IR spectra of the samples

3.5 XPS analysis

XPS analysis was performed for the ZCoENK sample to investigate the chemical state of the elements in the samples. Figure 6 (a-d) shows the XPS survey of ZnO-$CoFe_2O_4$, O 1s, Zn $2P_{2/3}$, Zn $2P_{1/2}$, Fe $2P_{2/3}$, Fe $2P_{1/2}$ and C 1s spectra which confirmed that Zn, Co and Fe elements had been formed by this procedure. The XPS spectrum of O 1s indicates that only one mode of oxygen is present on the surface of the sample. The peak located at a binding energy of 532.2 eV corresponds to the lattice oxygen of metal oxides. The peaks located at 1023.02 eV and 1045.98 eV in the XPS spectrum of Zn2p can be assigned to $2p_{3/2}$ and $2p_{1/2}$ spin orbit states, respectively. These present values are in agreement with the binding energy of Zn^{2+} ion of ZnO nanoparticles in the composite. The Co2p spectrum exhibited two weak peaks at approximately 774 and 790 eV. The XPS spectrum of Fe shows two peaks located at 710, and 718 eV for $2p_{3/2}$ and $2p_{1/2}$ corresponding to Fe^{3+} ion in spinel ferrite[23, 24].

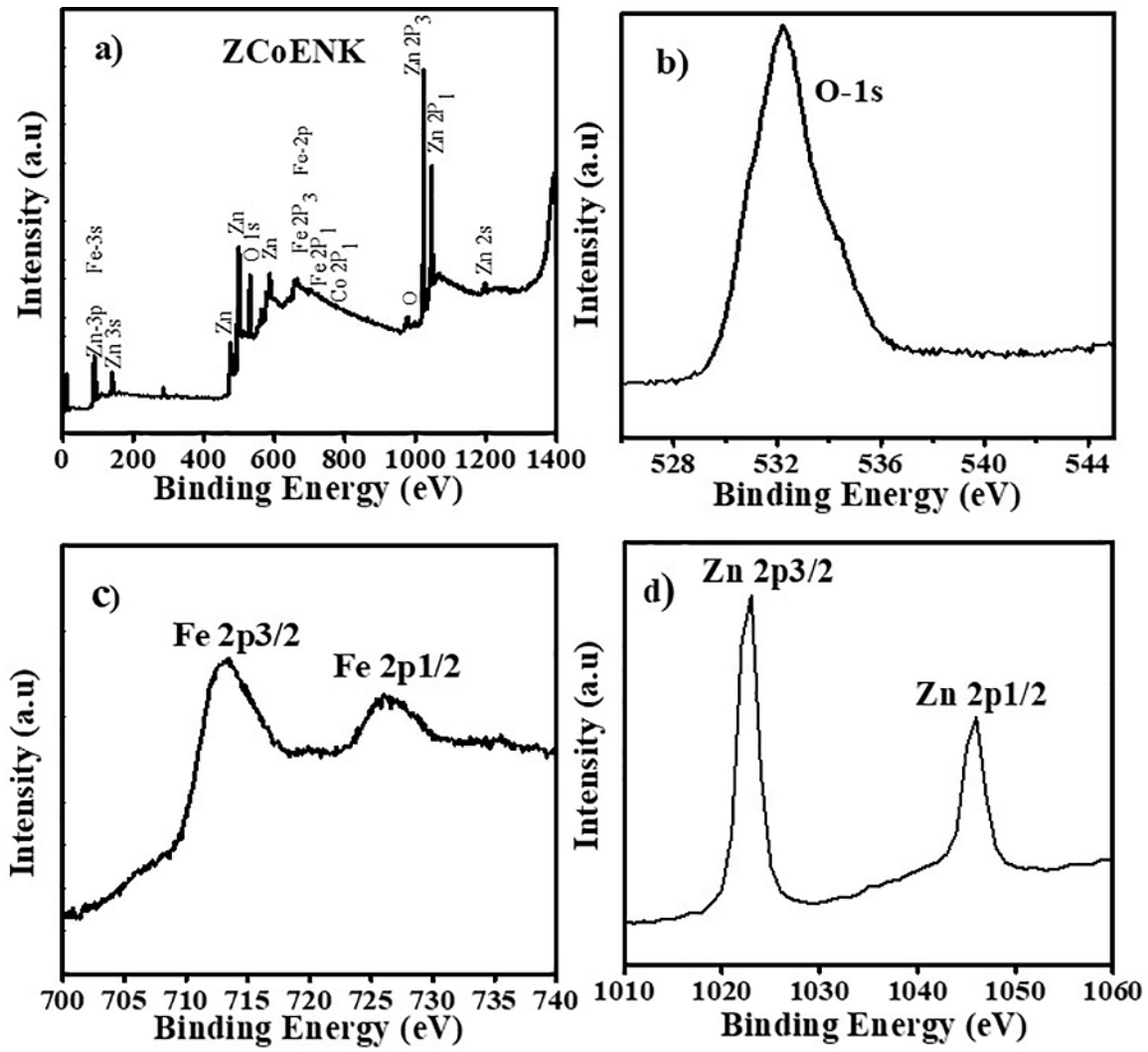

Figure 6. XPS spectra of ZCoENK

3.6 Photocatalytic Activity

The photocatalytic properties of the samples were evaluated by following degradation under solar light of the textile dye DR81 and the water-soluble dyes eluted from batik cloth. The extent of degradation of DR81 at different concentrations of the dye is shown in Figure 7a. The experiments were carried out under the following conditions: 20 mL of dye, 20 mg of composite, 2 h, and dye concentrations of 20-40 mg/L. At 30 mg/L dye concentration the composite samples show good catalytic activity with degradation reaching 93.6 and 99.6% for ZCoEN and ZCoENK, respectively. The increasing of dyes amount of do not have a significant effect on percent degradation because the increasing number of dye molecules in solution would prevent the distribution of light to the photocatalyst which results in a reduction in the amount of OH radicals. As well known, OH radicals are responsible for the degradation of dyes into simpler compounds[19].

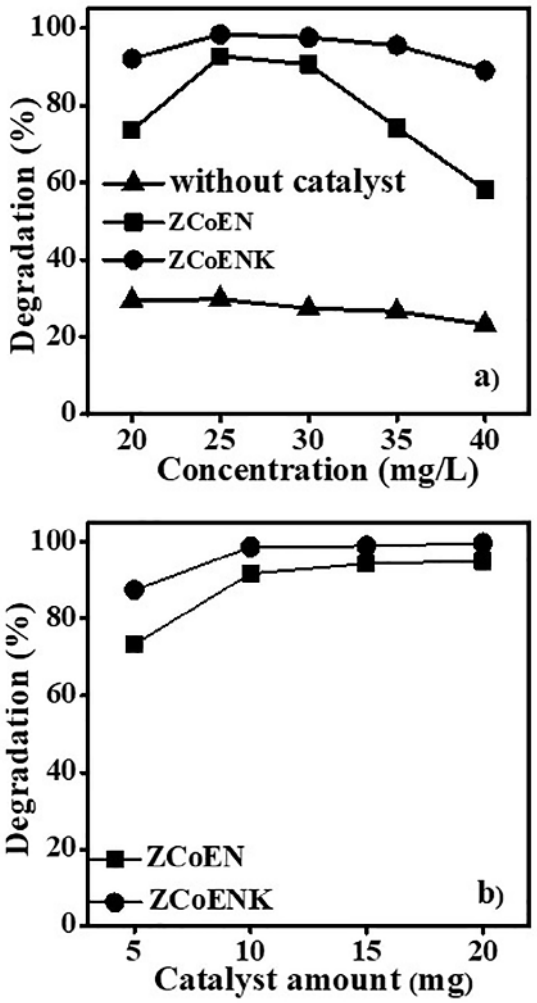

Figure 7. The effect of dye concentration a) and amount of catalyst b) on degradation of DR81 dye irradiated with solar light in the presence of ZCoEN or ZCoENK

ZCoEN sample has a significant decrease in degradation at 35 and 40 mg dye/L, meanwhile ZnO alone has lower activity (65.5%) compared with two composites because of its lower ability to absorb light in the visible region. In the absence of composite, only a few DR81 dyes were degraded under the present experimental conditions. It is clear ZnO-$CoFe_2O_4$ nanocomposites are better photocatalysts compare to that of ZnO due to the probability of a large number of electron hole pairs generated through the formation of OH radicals.

The higher activity of the ZCoENK than ZCoEN can be attributed to the morphology of a homogeneous sample with small particle size (SEM and TEM images). The smaller particle size of the sample has a good effect on the catalytic process because of the higher surface-to-volume ratio, contributes to surface area and more active sites which consequently leads to a higher interface interaction between the catalyst and the dye molecules, thus gives an impact on increasing the rate of degradation of dyes[22].

Figure 7b shows the effect of the amount of catalyst on degradation of dye for both composites. The experiments were conducted under the following conditions: 20 mL of dye, 25 mg/L dye concentration, 2 h irradiation time, and catalyst amounts of 5-20 mg. The graphs show that the degradation percentage increases with the increase in the amount of composites. The addition of excess catalysts did not have a significant effect on the increase in the degradation percentage. To be more efficient, the amount of catalyst used for subsequent work was 15 mg.

The mechanism of visible light photocatalysis can be explained as follows; it is known that ZnO is a n-type semiconductor and $CoFe_2O_4$ is an p-type semiconductor. When ZnO-$CoFe_2O_4$ heterojunction was irradiated by solar light, the electrons (e^-) in the valence band (VB) of dye sensitized ZnO and $CoFe_2O_4$ will be excited to the conduction band (CB) while the same number of holes (h^+) are left in the VB. The CB potential of ZnO is more positive than the $CoFe_2O_4$ while the VB potential of $CoFe_2O_4$ is more negative than the ZnO. The longer the irradiation time, the more number of excited electrons can move from the VB to the CB. Dissolved oxygen (O_2), acting as an electron scavenger, reacts with these electrons to yield active free radicals (•OH, O_2•$^-$, *etc*.). The holes will react with electron donors (H_2O) to yield active •OH free radicals. Subsequently, the surface adsorbed aromatic DR81 molecules are attacked by the h^+ and other free radicals leading to degradation and ring opening reactions[25, 26].

Figure 8a shows the degradation percentage of DR81 versus time in the presence of NCoEN, and NCoENK composites. The amount of degraded dyes increases with the increase in irradiation time, this is due to the amount of formed OH radicals increases. For large scale practical application of this catalyst, its long-term reuse is of economic significance[26].

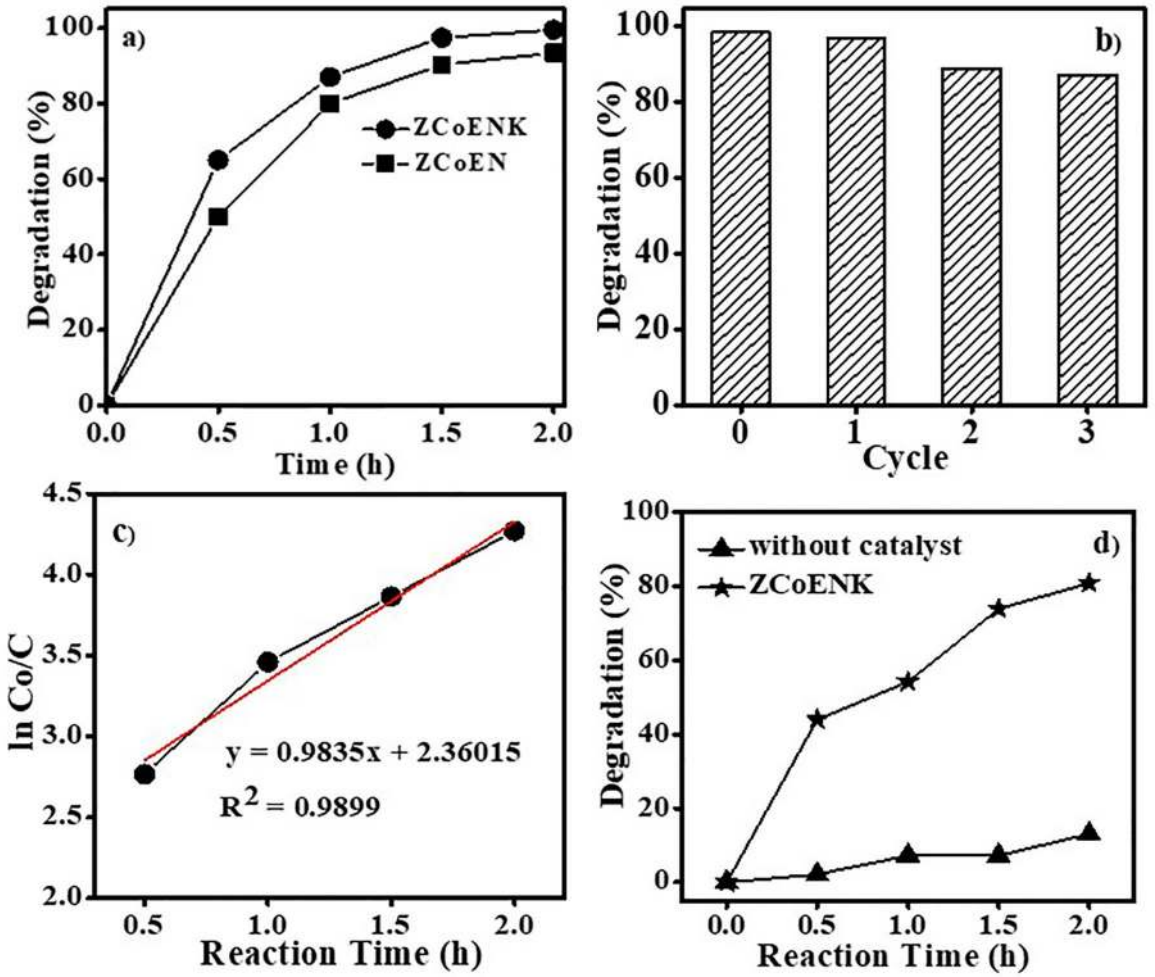

Figure 8. The degradation of DR81 dye a) over time in the presence of ZCoEN and ZCoENK, b) over 4 recycling experiments in the presence of ZCoENK, c) for calculation of the pseudo-first-order rate constant and d) the percentage degradation of batik cloth dyes in the presence of ZCoENK

To evaluate the photo stability and reusability of ZnO-$CoFe_2O_4$ (ZCoENK) samples, four successive recycling tests for degradation of DR81 solution were performed under solar light irradiation, as shown in Figure 8b. Between each cycle, the ZCoENK nanoparticles were recovered by filtration, washed with distilled water and dried at 105 °C. The degradation of DR81 by ZCoENK nanoparticles during the fourth cycle was 87%, a reduction of 11.4% compared to the first cycle. The loss of this activity could be due to the formation of microscopic aggregate during the recycling process as was observed previously[16].

The photocatalytic decomposition of DR81 on the surface of composites follows a pseudo-first-order kinetic law, expressed as:

$$\ln(Co/C) = kt \quad (4)$$

where C and Co are the reactant concentration at time t and t=0, respectively, k and t are the pseudo-first-order rate constant (reaction rate constant) and time, respectively[3]. The relationship between ln(C/Co) and irradiation time (reaction time) is shown in Figure 8c.

For the dyes in waste water from washing batik cloth, the activity of the nanocomposite ZCoENK was examined in the same way as DR81 (Figure 8d). Without a catalyst, the amount of degraded batik cloth dye was 13%, whilst the presence of the ZCoENK catalyst degraded 81% of the dye. This value is lower than the degradation percentage of DR81 because the dyes of batik cloth has more complex compounds than DR81 dye.

4. Conclusions

ZnO-$CoFe_2O_4$ magnetic nanocomposites were synthesized by hydrothermal method in the presence of rambutan fruit peel extract as capping agent. XRD patterns show the peaks corresponded to the structure of ZnO and $CoFe_2O_4$ in the composites. The nanocomposites absorb the visible light and have superparamagnetic so that they are potential to be used as a photocatalyst for dye degradation under solar light.

Furthermore, they can also be reused for the next process. The combination of homogeneous fine grains and conducive band gap of the nanocomposites have produced a good photocatalytic activity on degradation of DR81 and batik dyes in 2 h. Higher activity was obtained from the ZCoENK nanocomposite.

5. Acknowledgment

This work was supported by a KRPGB grant (contract number: 37/UN.16.17/PP.PGB/ LPPM/2018) from Andalas University.

6. References

1. Karunakaran C, JebaSing I, Vinayagamoorthy P. Synthesis of Superparamagnetic $ZnFe_2O_4$-Core/Ag-Deposited ZnO-shell Nanodiscs for Application as Visible Light Photocatalyst. *Journal of Nanoscience and Nanotechnology*. 2019;19(7):4064-4071.

2. Borgohain C, Senapati KK, Sarma KC, Phukan P. A facile synthesis of nanocrystalline $CoFe_2O_4$ embedded one-dimensional ZnO hetero-structure and its use in photocatalysis. *Journal of Molecular Catalysis A: Chemical*. 2012;363-364:495-500.

3. Falak P, Hassanzadeh-Tabrizi SA, Saffar-Teluri A. Synthesis, characterization, and magnetic properties of ZnO-$ZnFe_2O_4$ nanoparticles with high photocatalytic activity. *Journal of Magnetism and Magnetic Materials*. 2017;441:98-104.

4. Sun L, Shao R, Tang LQ, Chen Z. Synthesis of $ZnFe_2O_4$/ZnO nanocomposites immobilized on graphene with enhanced photocatalytic activity under solar light Irradiation. *Journal of Alloys and Compounds*. 2013;564:55-62.

5. Zheng J, Song X, Liu X, Chen W, Li Y, Guo J. Synthesis of hexagonal $CoFe_2O_4$/ZnO nanoparticles and their electromagnetic properties. *Materials Letters*. 2012;73:143-146.

6. Wilson A, Mishra SR, Gupta R, Ghosh K. Preparation and photocatalytic properties of hybrid core-shell reusable $CoFe_2O_4$-ZnO nanosphere. *Journal of Magnetism and Magnetic Materials*. 2012;324(17):2597-2601.

7. Sundararajan M, Sailaja V, Kennedy LJ, Vijaya JJ. Photocatalytic degradation of Rhodamine B under visible light using nanostructured zinc doped cobalt ferrite: Kinetics and mechanism. *Ceramics International*. 2017;43(1 Pt A):540-548.

8. Sathishkumar P, Pugazhenthiran N, Mangalaraja RV, Asiri AM, Anandan S. ZnO supported $CoFe_2O_4$ nanophotocatalysts for the mineralization of Direct Blue 71 in aqueous environments. *Journal of Hazardous Materials*. 2013;252-253:171-179.

9. Rahmayeni, Devi A, Stiadi Y, Jamarun N, Emriadi, Arief S. Preparation, characterization of ZnO/$CoFe_2O_4$ magnetic nanocomposites and activity evaluation under solar light irradiation. *Journal of Chemical and Pharmaceutical Research*. 2015;7(9S):139-146.

10. Castro TJ, da Silva SW, Nakagomi F, Moura NS, Franco AJ Jr, Morais PC. Structural and magnetic properties of ZnO-$CoFe_2O_4$ nanocomposites. *Journal of Magnetism and Magnetic Materials*. 2015;389:27-33.

11. Senthilkumar SR, Sivakumar T. Green tea (*Camellia Sinensis*) mediated synthesis of zinc oxide (ZnO) nanoparticles and studies on their antimicrobial activities. *International Journal of Pharmacy and Pharmaceutical Sciences*. 2014;6(6):461-465.

12. Manikandan A, Sridhar R, Antony SA, Ramakrishna S. Simple *Aloe vera* plant-extracted microwave and conventional combustion synthesis: Morphological, optical, magnetic and catalytic properties of $CoFe_2O_4$ nanostructures. *Journal of Molecular Structure*. 2014;1076:188-200.

13. Bhuyan T, Mishra K, Khanuja M, Prasad R, Varma A. Biosynthesis of Zinc oxide nanoparticles from *Azadirachta indica* for antibacterial and photocatalytic applications. *Materials Science in Semiconductor Processing*. 2015;32:55-61.

14. Ramesh M, Anbuvannan M, Viruthagiri G. Green synthesis of ZnO nanoparticles using *Solanum nigrum* leaf extract and their antibacterial activity. *Spectrochimica Acta Part A: Molecular and Biomolecular Spectroscopy*. 2015;136(Pt B):864-870.

15. Yuvakkumar R, Suresh J, Nathanael AJ, Sundrarajan M, Hong SI. Rambutan (*Nephelium Lappaceum* L.) peel extract assisted biomimetic synthesis of nickel oxide nanocrystals. *Materials Letters*. 2014;128:170-174.

16. Karnan T, Selvakumar SAS. Biosynthesis of ZnO nanoparticles using rambutan (*Nephelium lappaceum* L.) peel extracts and their photocatalytic activity on methyl orange dye. *Journal of Molecular Structure*. 2016;1125:358-365.

17. Rahmayeni, Ramadani A, Stiadi Y, Jamarun N, Emriadi, Arief S. Photocatalytic Performance of ZnO-$ZnFe_2O_4$ Magnetic Nanocomposites on Degradation of Congo Red Dye Under Solar Light Irradiation. *Journal of Materials and Environmental Sciences*. 2017;8(5):1634-1643.

18. Sagadevan S, Chowdhury ZZ, Rafique RF. Preparation and Characterization of Nickel ferrite Nanoparticles via Co-precipitation Method. *Materials Research*. 2018;21(2):e20160533.

19. Lamba R, Umar A, Mehta SK, Kansal SK. CeO_2-ZnO hexagonal nanodisks: Efficient material for the degradation of direct blue 15 dye and its simulated dye bath effluent under solar light. *Journal of Alloys and Compounds*. 2015;620:67-73.

20. Guo X, Zhu H, Li Q. Visible-light-driven photocatalytic properties of ZnO/$ZnFe_2O_4$ core/shell nanocable arrays. *Applied Catalysis B: Environmental*. 2014;160-161:408-414.

21. Mathubala G, Manikandan A, Antony SA, Ramar P. Photocatalytic degradation of methylene blue dye and magneto-optical studies of magnetically recyclable spinel $Ni_xMn_{1-x}Fe_2O_4$ (x = 0.0–1.0) nanoparticles. *Journal of Molecular Structure*. 2016;1113:79-87.

22. Stan M, Popa A, Toloman D, Dehelean A, Lung I, Katona G. Enhanced photocatalytic degradation properties of zinc oxide nanoparticles synthesized by using plant extracts. *Materials Science in Semiconductor Processing*. 2015;39:23-29.

23. Long NV, Yang Y, Teranishi T, Thi CM, Cao Y, Nogamie M. Related magnetic properties of $CoFe_2O_4$ cobalt ferrite particles synthesized by the polyol method with $NaBH_4$ and heat treatment: new micro and nanoscale structures. *RSC Advances*. 2015;5(70):56560-56569.

24. Zhao Y, Lin C, Bi H, Liu Y, Yan Q. Sol-gel based hydrothermal method for the synthesis of 3D flower-like ZnO microstructures composed of nano sheets for photocatalytic applications. *Applied Surface Science*. 2017;392:701-707.

25. Adeleke JT, Theivasanthi T, Thiruppathi M, Swaminathan M, Akomolafe T, Alabi AB. Photocatalytic degradation of methylene blue by ZnO/$NiFe_2O_4$ nanoparticles. *Applied Surface Science*. 2018;455:195-200.

26. Zhu HY, Jiang R, Fu YQ, Li RR, Yao J, Jiang ST. Novel multi-functional $NiFe_2O_4$/ZnO hybrids for dye removal by adsorption, photo catalysis and magnetic separation. *Applied Surface Science*. 2016;369:1-10.